

NACA RM L53K27

7508



TECH LIBRARY KAFB, NM



RESEARCH MEMORANDUM

WIND-TUNNEL INVESTIGATIONS AT LOW AND TRANSONIC SPEEDS OF
THE FEASIBILITY OF SELF-ACTUATING SPOILERS AS A
LATERAL-CONTROL DEVICE FOR A MISSILE

By Harleth G. Wiley and William C. Hayes, Jr.

Langley Aeronautical Laboratory
Langley Field, Va.

NATIONAL ADVISORY COMMITTEE
FOR AERONAUTICS

WASHINGTON

January 28, 1954

Classification cancelled (or changed to) Unclassified

By Authority: Nasa Tech Pub Announcement #122
(OFFICER AUTHORIZED TO CHANGE)

By.....

3 Dec 51

GRADE OF OFFICER MAKING CHANGE)

29 Mar 61

DATE



0144284

NACA RM L53K27

~~CONFIDENTIAL~~

NATIONAL ADVISORY COMMITTEE FOR AERONAUTICS

RESEARCH MEMORANDUM

WIND-TUNNEL INVESTIGATIONS AT LOW AND TRANSONIC SPEEDS OF
THE FEASIBILITY OF SELF-ACTUATING SPOILERS AS A
LATERAL-CONTROL DEVICE FOR A MISSILE

By Harleth G. Wiley and William C. Hayes, Jr.

SUMMARY

Investigations were made in the Langley 300 MPH 7- by 10-foot tunnel and on the transonic bump of the Langley high-speed 7- by 10-foot tunnel to determine the feasibility of a self-actuating spoiler as a lateral-control device for a missile having a 60° delta wing. The lateral-control characteristics of various sizes of plain and cambered spoilers on a 60° delta wing were determined through an angle-of-attack range of -4° to 20° at low speeds. The aerodynamic moments acting on two cambered spoilers were determined through an angle of rotation range of 0° to 180° at Mach numbers of about 0.6 to 1.08.

Results indicated that such a system will provide control at low speeds throughout an angle-of-attack range of 0° to about 12° for all spoiler configurations tested and that positive rotational moments will be obtained throughout the angle-of-rotation range up to a Mach number of 1.08.

INTRODUCTION

Simplification of the control system of airplanes and guided missiles by eliminating or reducing the complexity of the control power system offers the advantages of lower cost and higher reliability of the airframe. One type of control that appears promising from the standpoint of simplicity, derives its motive power from the energy of the airstream.

In order to implement a recently proposed missile control philosophy in which the missile seeks the target in a constantly correcting rolling motion (refs. 1 and 2), a simplified lateral control has been devised which utilizes aerodynamic forces to position spoilers as required. The control system comprises a spoiler vane on the upper and lower surfaces

~~CONFIDENTIAL~~~~14-00000~~

of each wing, with the vanes oriented 90° to each other on a common shaft such that one tends to spoil the wing flow while the companion vane is aligned with the airstream.

In order to determine the feasibility of these self-actuating spoilers as a missile lateral-control system, tests of several aspects of such a system were made by the National Advisory Committee for Aeronautics.

Reported herein are the results of tests at low speeds in the Langley 300 MPH 7- by 10-foot tunnel of the lateral-control effectiveness of self-actuating spoilers with varying spoiler vane chords, span lengths, and streamwise camber. All spoilers tested on the 60° delta wing were mounted with the spoiler-shaft center lines at 37.5 percent wing semispan and at 82 percent wing root chord and were designed according to the recommendations of reference 3. Tests were made at 0° angle of sideslip through an angle-of-attack range of -4° to about 20° . Brief tests were also made of "spoiler-free" actuating times for several cambered spoiler configurations.

Presented also are results of tests made on the transonic bump of the Langley high-speed 7- by 10-foot tunnel to determine the aerodynamic moments acting on two isolated spoiler configurations through an angle-of-rotation range of 0° to 180° .

COEFFICIENTS AND SYMBOLS

Results of the tests of self-actuating spoiler control effectiveness on a 60° delta wing are presented as standard NACA coefficients of forces and moments about the stability axes as presented in figure 1. The orientation of axes to which the aerodynamic moments on an isolated spoiler are referred is presented in figure 2. Coefficients and symbols used herein are defined as follows:

C_L lift coefficient, $\frac{\text{Lift}}{qS}$

C_D drag coefficient, $\frac{\text{Drag}}{qS}$

C_m pitching-moment coefficient, $\frac{\text{Pitching moment referred to } 0.25\bar{c}}{qS\bar{c}}$

~~CONFIDENTIAL~~

- C_l rolling-moment coefficient,

$$\frac{\text{Rolling moment of spoiler and wing} - \text{Rolling moment of wing alone}}{qSb}$$
- C_n yawing-moment coefficient,

$$\frac{\text{Yawing moment of spoiler and wing} - \text{Yawing moment of wing alone}}{qSb}$$
- C_R rotational-moment coefficient of spoiler,

$$\frac{\text{Rotational moment about Z-axis of spoiler}}{qS_S c_S}$$
- C_B bending-moment coefficient of spoiler,

$$\frac{\left\{ \left[(\text{Bending moment about spoiler X-axis})^2 + (\text{Bending moment about spoiler Y-axis})^2 \right]^{1/2} \right\}}{qS_S b_S}$$
- S wing area, 6.93 sq ft
- \bar{c} mean aerodynamic chord of wing, $\frac{2}{S} \int_0^{b/2} c^2 dy$, 2.31 ft
- c_r root chord of wing, 3.46 ft
- c_t tip chord of wing, 0
- c local wing chord, ft
- b span of wing, 4.00 ft
- y distance along wing span, ft
- S_S spoiler vane area, sq ft
- c_S chord of spoiler (measured in plane perpendicular to Z-axis of spoiler), ft
- b_S span of spoiler (measured along Z-axis of spoiler), ft
- y_S distance along spoiler vane chord, ft

- V free-stream air velocity, ft/sec
- ρ mass density of air, slugs/cu ft
- q free-stream dynamic pressure, $\frac{1}{2}\rho V^2$, lb/sq ft
- M Mach number
- M_a average local Mach number
- R Reynolds number of wing based on \bar{c}
- R_s Reynolds number of spoiler based on y_s
- α angle of attack of wing, deg
- δ angle of spoiler rotation (measured from plane of X- and Z-axes of spoiler to reference line of spoiler, positive when clockwise), deg

MODELS AND APPARATUS

The 60° delta wing on which the spoilers were mounted for the low-speed tests was the same wing used in reference 3 and had an aspect ratio of 2.31, a taper ratio of 0, and was constructed of a 5/8-inch-thick flat steel plate with beveled leading and trailing edges (fig. 3).

The dimensions of the 1/8-inch-thick aluminum vanes of spoilers tested at low speeds on the 60° delta wing, hereinafter referred to as spoilers 1 to 8, are presented in figure 4 and table I. Each complete spoiler assembly consisted of two spoiler vanes oriented at right angles to each other and mounted on a common 3/8-inch-diameter steel shaft which extended through the wing perpendicular to the wing chord plane. A complete spoiler assembly was mounted on ball bearings on each wing semispan at the 0.375-semispan station and at 0.82 wing root chord. (For the control-effectiveness tests the spoilers were locked so that the upper-surface vane of the spoiler on the right wing semispan was perpendicular to the airstream while the corresponding vane on the left semispan was parallel to the airstream.) Spoilers 1 to 4 had plain flat vanes with oppositely beveled leading and trailing edges. Spoilers 5 to 8 were cambered in order to utilize aerodynamic forces to provide more positive autorotation (fig. 4).

For low-speed tests of actuation time for spoilers 5, 6, 7, and 8, electrical contacts were installed 90° apart on the wing and were connected to a recording potentiometer. Records were thus made of the

time required for a 90° rotation of the spoiler from the unspoiling or "off" position on the upper surface of the wing to the spoiling or "on" position.

The model was tested on the single support strut of the Langley 300 MPH 7- by 10-foot tunnel and was attached to the tunnel balance system for measurement of aerodynamic forces and moments. A small fuselage was used on the model to cover the support strut linkages.

The details and dimensions of spoilers 9 and 10 which were tested as isolated half-spoilers on the transonic bump in the Langley high-speed 7- by 10-foot tunnel are presented in figure 5 and table I. These spoilers consisted of single brass vanes welded to a 1/2-inch-diameter steel shaft which extended through a rubber-gasketed hole in the cover plate of the bump. The shaft was attached to a five-component electrical strain-gage balance mounted beneath the bump surface. Aerodynamic forces and moments of the spoiler were read on a calibrated potentiometer.

TESTS AND CORRECTIONS

Tests of spoiler lateral-control effectiveness were made in the Langley 300 MPH 7- by 10-foot tunnel at a dynamic pressure q of 56 pounds per square foot, corresponding to a Mach number of about 0.2 and a Reynolds number, based on the mean aerodynamic chord of the wing, of about 3×10^6 . The tests were made at an angle of sideslip of 0° and through an angle-of-attack range of -4° to about 20° . Tests of spoiler actuation times were made at dynamic pressures of 25 and 56 pounds per square foot with the wing at 0° angle of attack.

Corrections for tunnel blockage and buoyancy were negligible and were therefore not applied to these data.

Tests to determine rotational- and bending-moment characteristics of isolated spoilers were made in the Langley high-speed 7- by 10-foot tunnel utilizing the high-velocity flow field generated over the curved surface of a bump located on the tunnel floor. Typical local Mach number contours with the models removed, but with model positions superimposed on the charts, are shown in figure 6. The effective test Mach number was obtained from contour charts similar to those of figure 6 by

using the relationship $M = \frac{1}{S_s} \int_0^{b_s} c_s M_a dy_s$. Reynolds number for the

tests on the transonic bump, based on the chord of the spoiler varied with Mach number from about 0.6×10^6 to 0.8×10^6 (fig. 7). The isolated spoiler models were tested through an angle-of-rotation range of 0° to 180° .

RESULTS AND DISCUSSION

The low-speed aerodynamic characteristics of the plain wing (fig. 8) were presented and discussed in detail in reference 3. The variation of rolling-moment and yawing-moment coefficients with angle of attack at low speeds for spoilers 1 to 8 are presented in figures 9 and 10 and the variations of spoiler actuating times are presented in figure 11. The variations of spoiler rotational-moment coefficients with angle of rotation at transonic speeds are presented in figures 12 and 13 with the variations of spoiler bending-moment coefficients with angle of rotation presented in figure 14.

Rolling-Moment Coefficients

Spoilers 1 to 4 provided favorable rolling-moment coefficients through an angle-of-attack range of -4° to 12° , with spoilers 3 and 4, having vane spans of 0.15c and 0.25c, respectively, providing the greatest rolling effectiveness (fig. 9). (Lateral-control characteristics are presented in this paper for the "right-roll" condition with the upper-surface spoiler vane on the right wing oriented perpendicular to the airstream. The other or "left-roll" condition results in a negative reflection of the "right-roll" condition.) The cambered spoilers with somewhat less vane area than plain spoilers 1 to 4 provided lower but still favorable rolling moments up to an angle of attack of about 12° (fig. 10). Spoiler 7 with a vane chord of $0.09b/2$ and a span of 0.15c had the highest rolling effectiveness of the cambered spoilers. (Although spoilers 6 and 7 had generally similar vane dimensions, spoiler 6, with greater camber, had considerably less rolling effectiveness than did spoiler 7. The increased camber of spoiler 6 resulted in increased frontal area of the vane on the lower surface thus spoiling the flow on the lower surface of the wing and decreasing the overall rolling effectiveness.)

Yawing-Moment Coefficients

The yawing-moment coefficients for all spoilers tested were generally unfavorable through the angle-of-attack range of 0° to 12° (figs. 9 and 10). The unfavorable yawing-moment coefficients apparently result from the presence of a spoiler on both the upper surface of the right wing and the lower surface of the left wing.

Spoiler Actuating Times

Brief tests at low speeds indicated that plain spoilers 1, 2, 3, and 4, with oppositely beveled leading and trailing edges, would not

autorotate satisfactorily. Spoilers 5, 6, 7, and 8 were therefore built to incorporate various amounts of camber in order to provide greater aerodynamic rotational moments. The time required for 90° rotation of the spoiler from the "off" position (upper surface vane aligned with airstream) to the "on" (upper vane perpendicular to airstream), for spoilers 5, 6, 7, and 8, at dynamic pressures of 25 and 56 pounds per square foot, is presented in figure 11. Of the four spoilers tested, spoiler 7 consistently required the least time for 90° of rotation. The times required for 90° of spoiler rotation, are of course, functions of aerodynamic rotational moment, spoiler moment of inertia, aerodynamic damping, and bearing friction. Simple calculations using the rotational-moment characteristics of spoiler 9 (fig. 13) and the calculated moment of inertia, show that the predominant effects on spoiler rotational time result from aerodynamic rotational moment and from moment of inertia.

Spoiler Rotational-Moment Coefficients

On the basis of results of low-speed tests of lateral-control characteristics and spoiler rotational times (figs. 9, 10, and 11), spoiler 7 was selected as the most favorable configuration and was modified to form spoilers 9 and 10 for determination of isolated-spoiler characteristics at transonic speeds. (The isolated-spoiler data are considered to be applicable for a spoiler in the presence of a complete wing at 0° angle of attack.) The variations of rotational-moment coefficients (moment tending to rotate the spoiler) with angle of rotation at several Mach numbers are presented in figure 12 for isolated single vanes of spoilers 9 and 10. Negative rotational-moment coefficients were obtained over part of the spoiler rotational range for both spoilers 9 and 10 when considered as single-vane spoilers (fig. 12). Summations of rotational-moment coefficients for complete spoiler configurations for spoilers 9 and 10 are presented in figure 13. (The characteristics of the complete spoiler were obtained by algebraic addition, with a 90° phase displacement, of the rotational-moment coefficients of similar upper- and lower-surface vanes.) Positive spoiler rotational-moment coefficients were obtained for spoilers 9 and 10 throughout the angle-of-rotation range for all Mach numbers investigated (fig. 13).

Spoiler Bending-Moment Coefficients

The variations of bending-moment coefficients C_B with angle of rotation at Mach numbers of 0.6 and 0.8 for a single vane of spoiler 9 are presented in figure 14. The bending-moment coefficients as presented are indicative of the structural loads at the root of the spoiler shaft.

CONCLUSIONS

From results of tests to determine the feasibility of self-actuating spoilers as lateral-control devices on a missile, the following conclusions may be drawn.

1. Favorable rolling-moment coefficients were obtained at low speeds over an angle-of-attack range of 0° to about 12° for all plain and cambered self-actuating spoilers investigated on a thin 60° delta wing.

2. At low speeds on a 60° delta wing, positive rotational tendencies were obtained only for cambered spoilers. At Mach numbers up to 1.08, results indicated that positive rotational-moment coefficients can be obtained throughout an angle-of-rotation range of 0° to 180° .

Langley Aeronautical Laboratory,
National Advisory Committee for Aeronautics,
Langley Field, Va., November 12, 1953.

REFERENCES

1. Curfman, Howard J., Jr., Strass, H. Kurt, and Crane, Harold L.: Investigations Toward Simplification of Missile Control Systems. NACA RM L53I21a, 1953.
2. Gardiner, Robert A.: A Combined Aerodynamic and Guidance Approach for a Simple Homing System. NACA RM L53I10a, 1953.
3. Wiley, Harleth G., and Solomon, Martin: A Wind-Tunnel Investigation at Low Speeds of the Aerodynamic Characteristics of Various Spoiler Configurations on a Thin 60° Delta Wing. NACA RM L52J13, 1952.

TABLE I.- COORDINATES FOR SPOILER CAMBER

[All dimensions in inches unless otherwise noted]

Spoiler 5

y_s	x
0	0
.1	0
.2	0
.3	0
.4	0
.5	0
.6	0
.7	0
.8	0
.9	0
1.0	0
1.1	.02
1.2	.05
1.3	.08
1.4	.11
1.5	.14
1.6	.17
1.7	.22
1.8	.27
1.9	.33
2.0	.39
2.1	.45
2.2	.52
2.3	.59
2.4	.68
2.5	.72

Spoiler 6

y_s	x
0	0
.1	0
.2	0
.3	0
.4	.01
.5	.04
.6	.10
.7	.17
.8	.30
.9	.42
.95	.56

Spoilers 9
and 10

y_s	x
0	0
.1	0
.2	0
.3	0
.4	.01
.5	.04
.6	.08
.7	.13
.8	.20
.9	.29
1.0	.38

Spoilers 7
and 8

y_s	x
0	0
.1	0
.2	0
.3	0
.4	0
.5	0
.6	.02
.7	.06
.8	.10
.9	.15
1.0	.20
1.1	.25

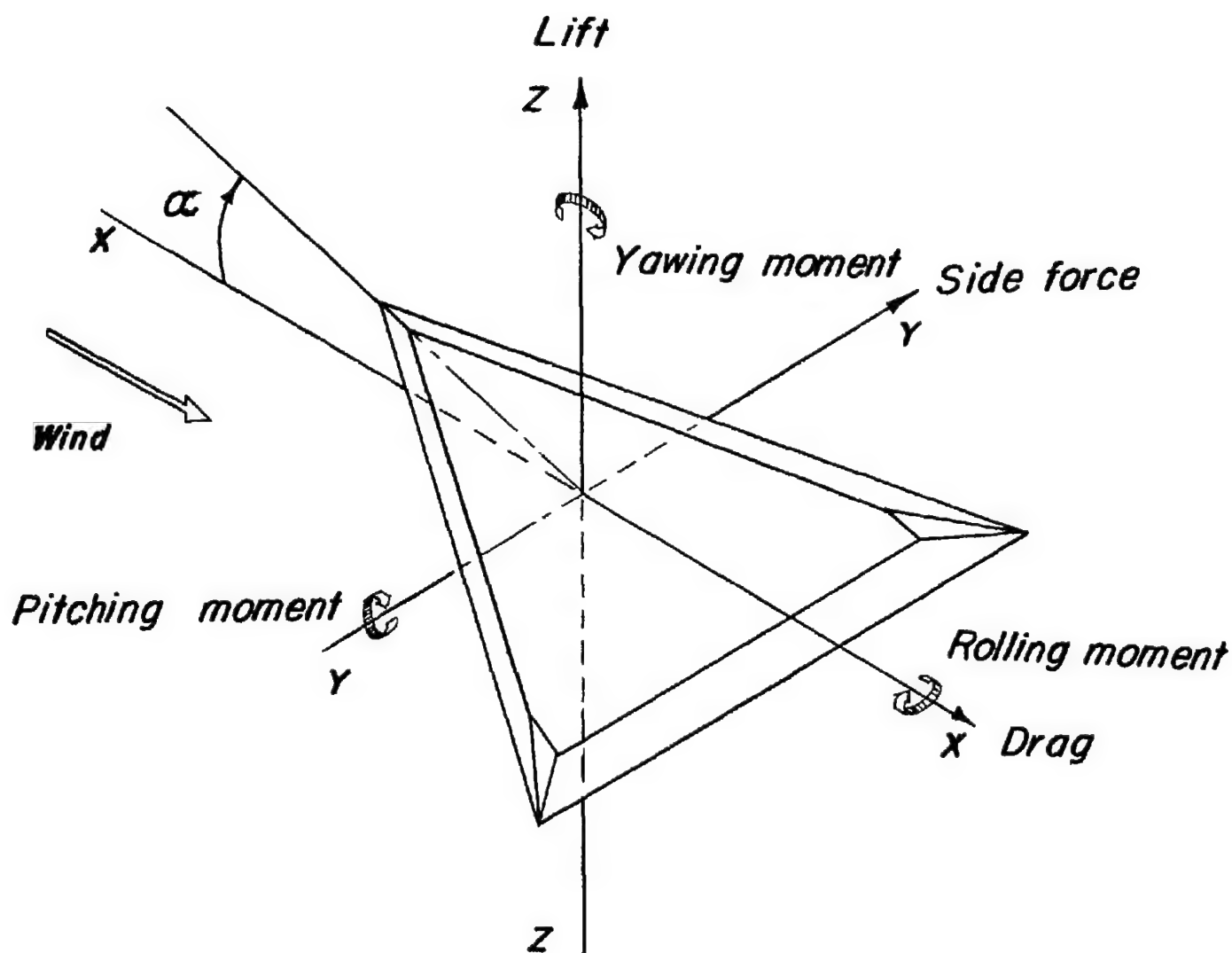


Figure 1.- System of stability axes. Positive values of forces, moments, and angles are indicated by arrows.

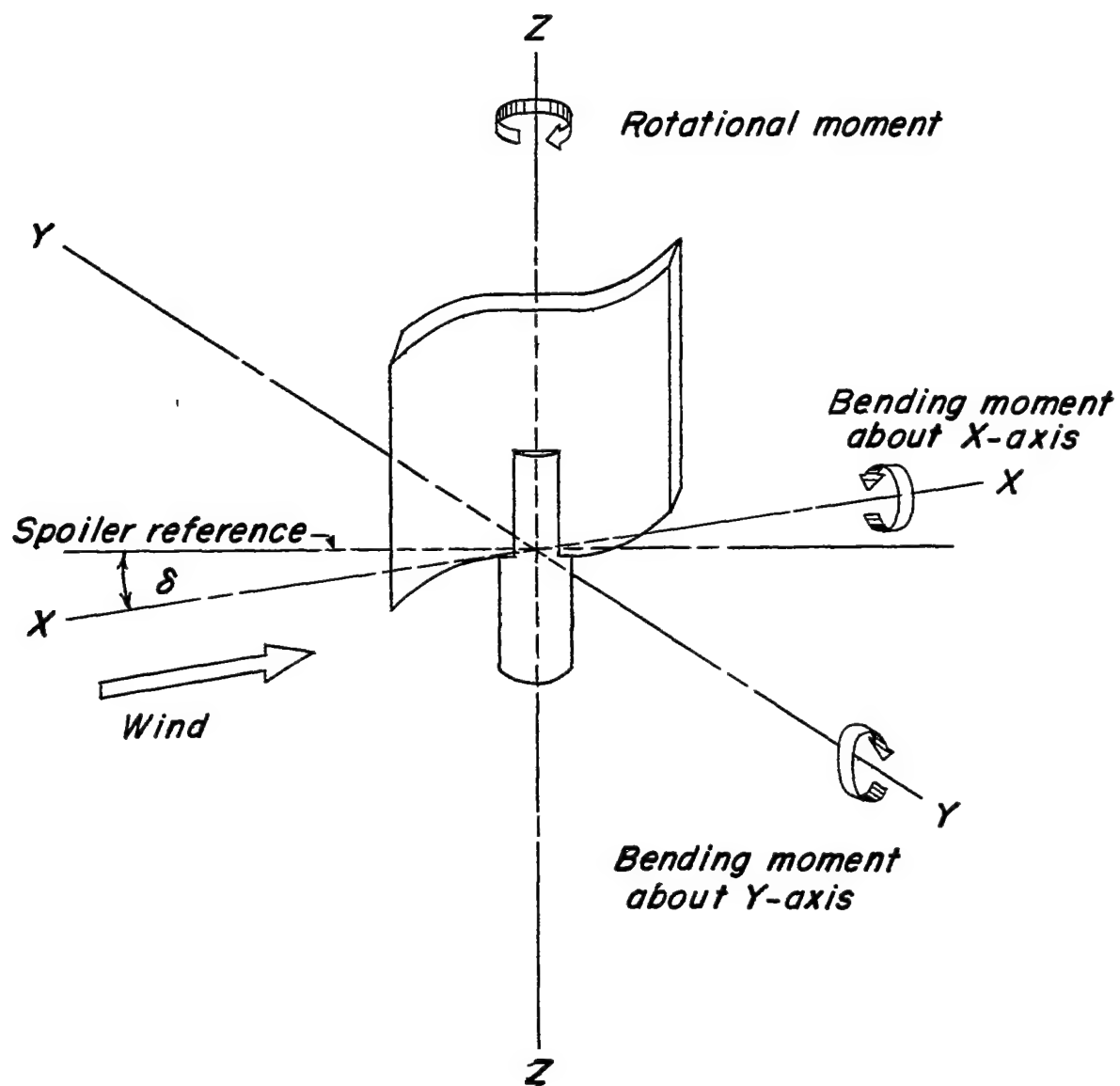


Figure 2.- System of spoiler axes. (Positive direction of moments indicated by arrows.)

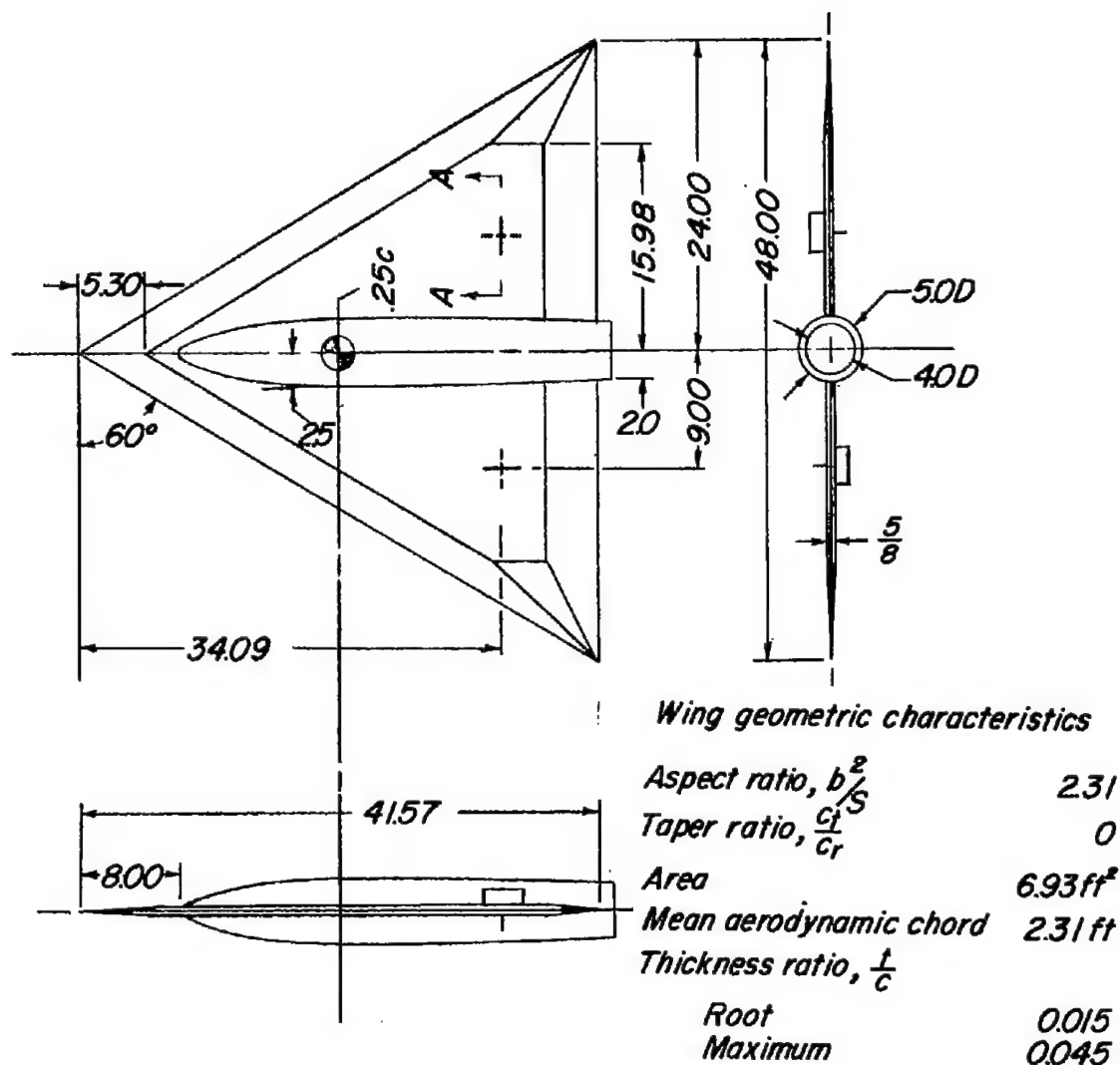


Figure 3.- Sketch of 60° delta wing showing location of spoilers. (All dimensions are in inches unless otherwise noted.)

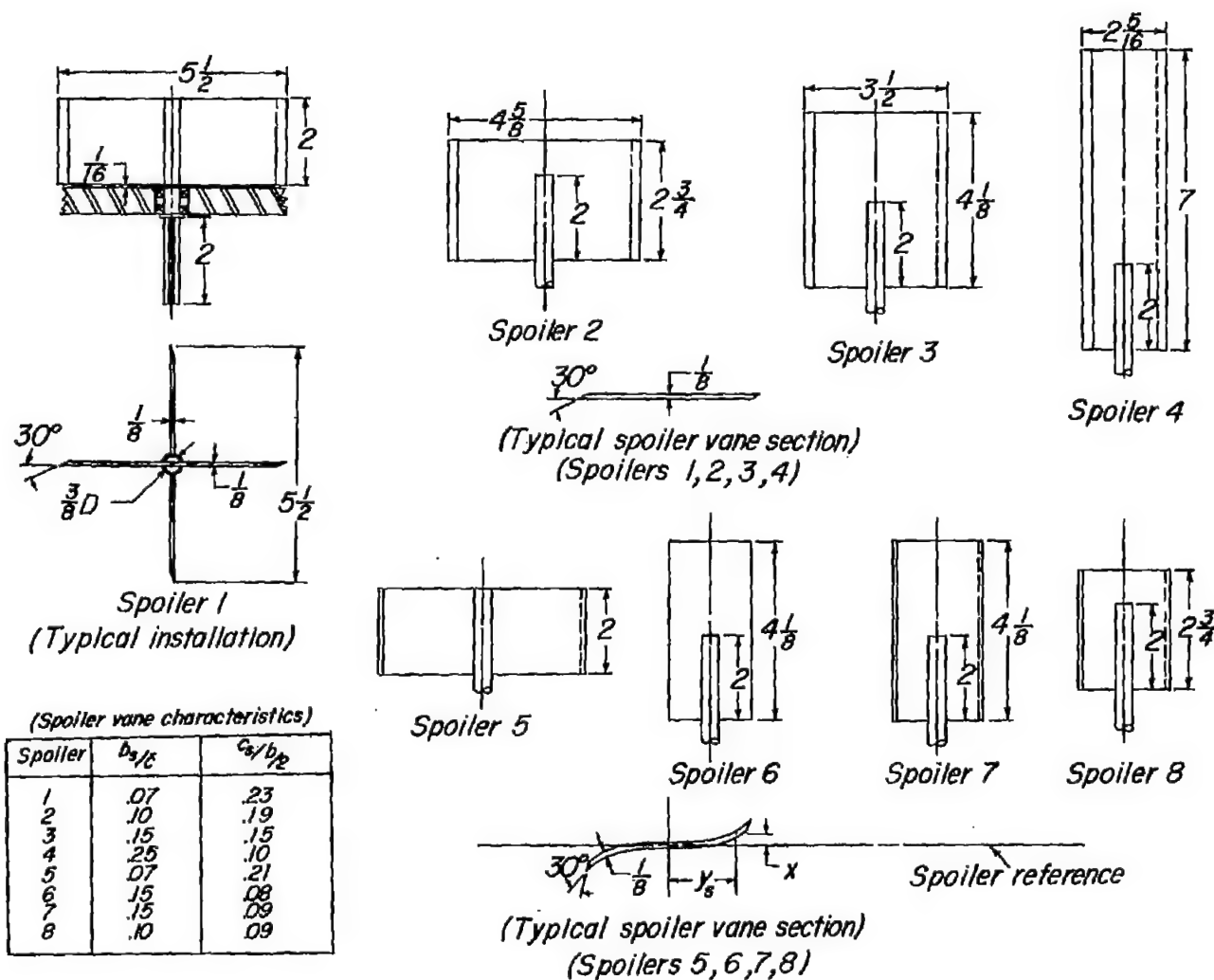


Figure 4.- Details of plain and cambered spoilers tested on 60° thin delta wing. (Coordinates of cambered spoilers are presented in table I. All dimensions in inches unless otherwise specified.)

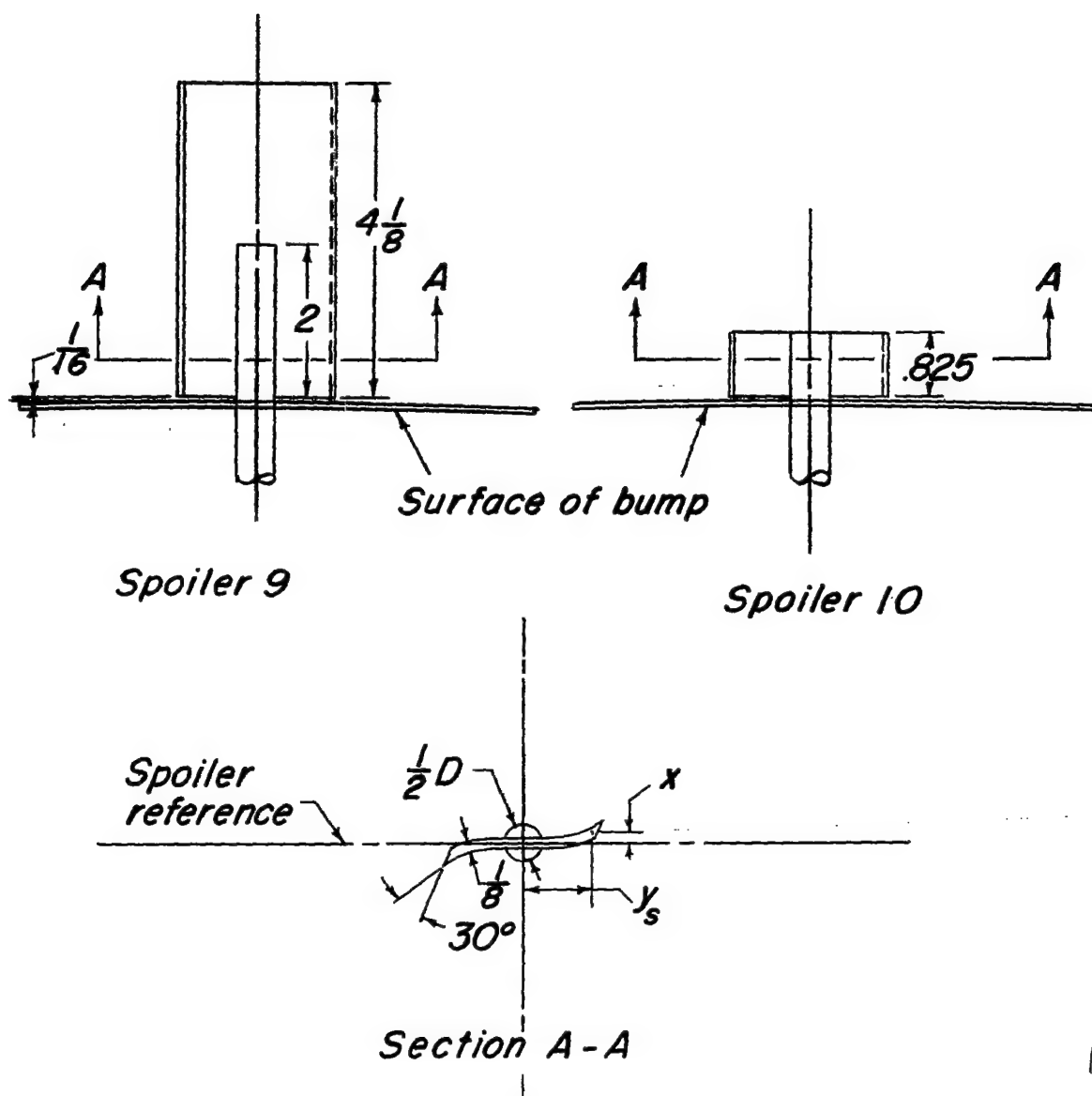


Figure 5.- Details of spoiler configurations tested on transonic bump.
(Coordinates presented in table I. All dimensions in inches unless
otherwise specified.)

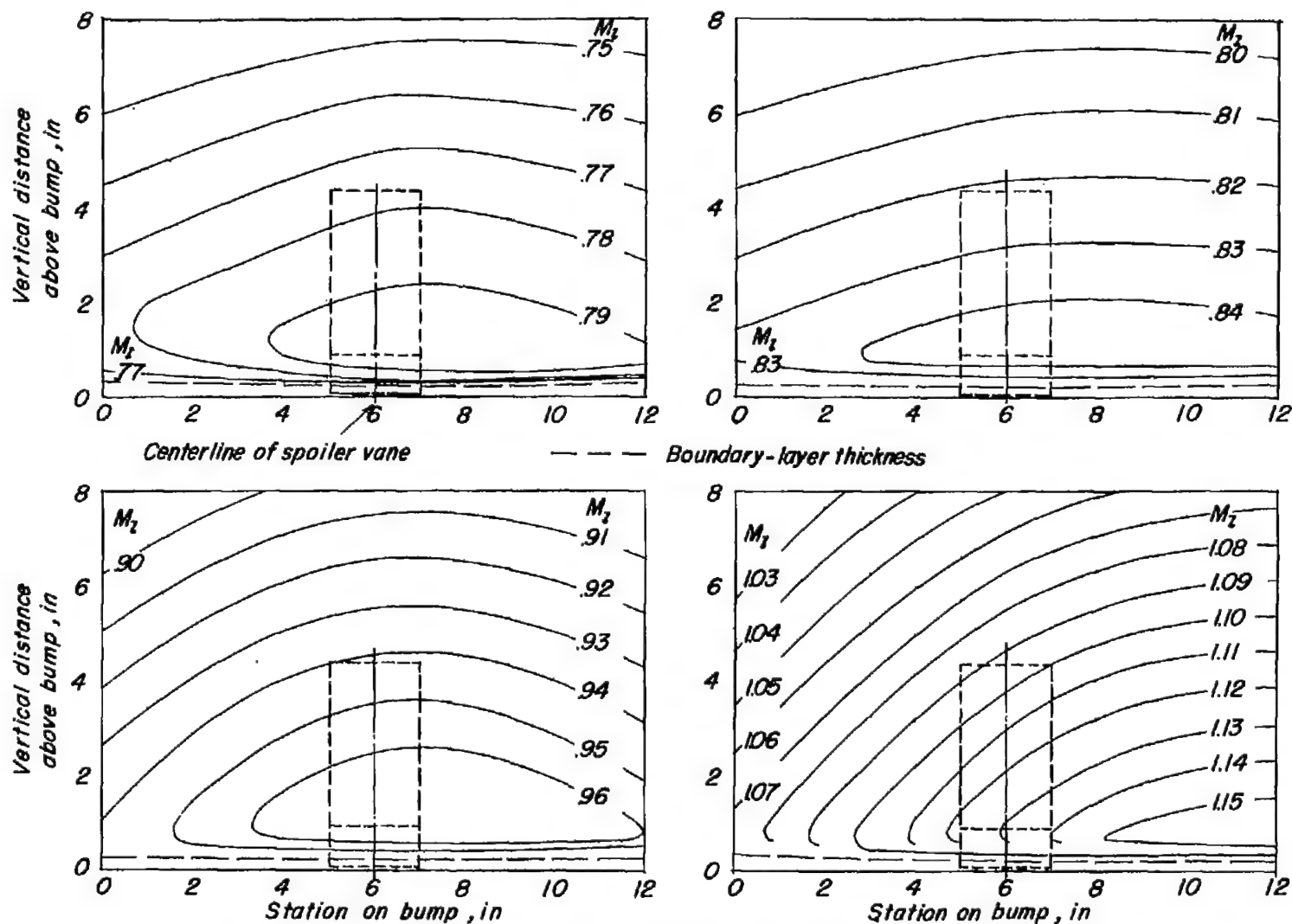


Figure 6.- Typical Mach number contours over transonic bump in region of model location.

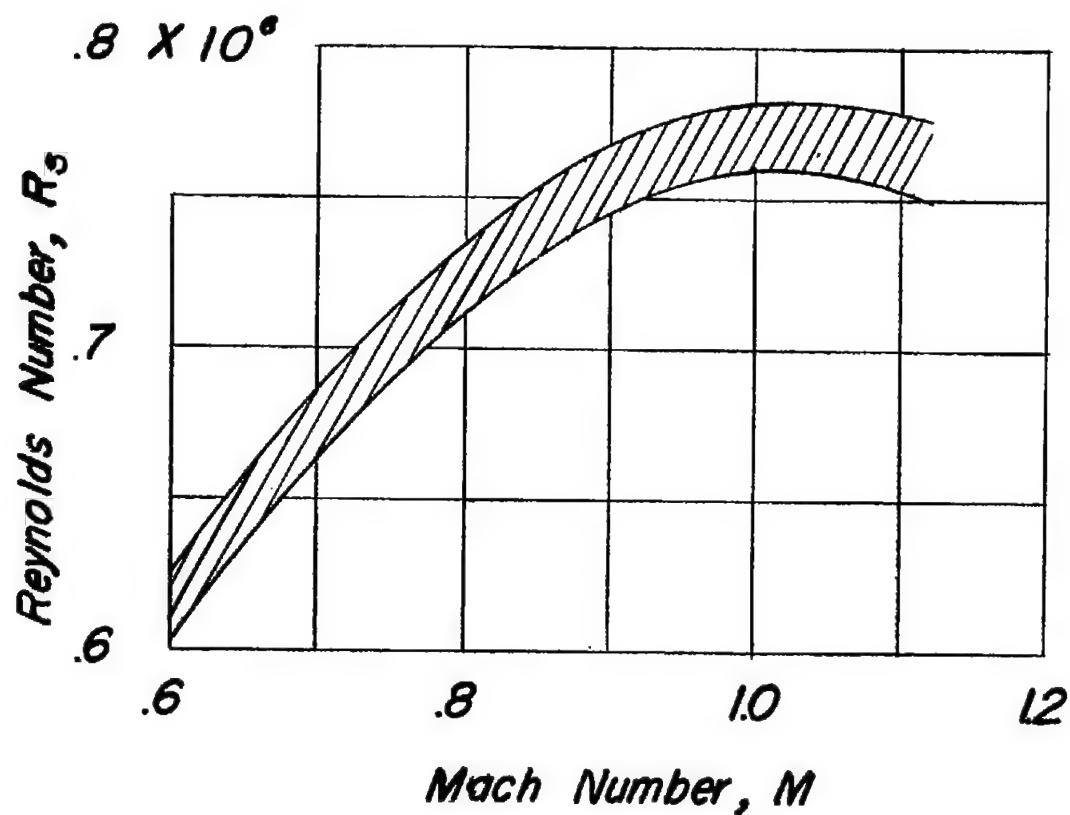


Figure 7.- Variation of Reynolds number with Mach number for spoilers tested on the transonic bump.

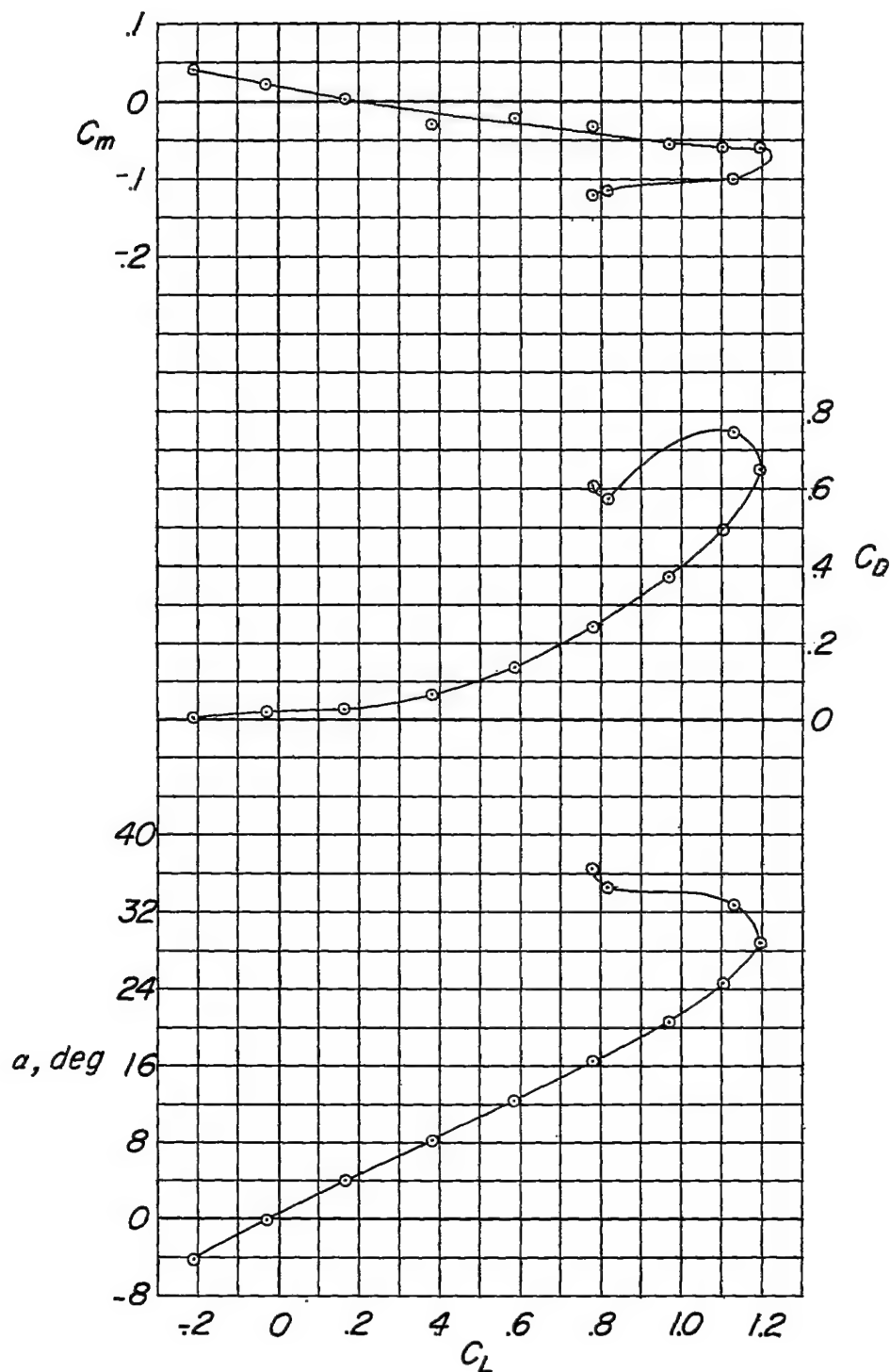


Figure 8.- The aerodynamic characteristics of a plain 60° delta wing with an aspect ratio of 2.31, taper ratio of 0, and constant-thickness airfoil section.

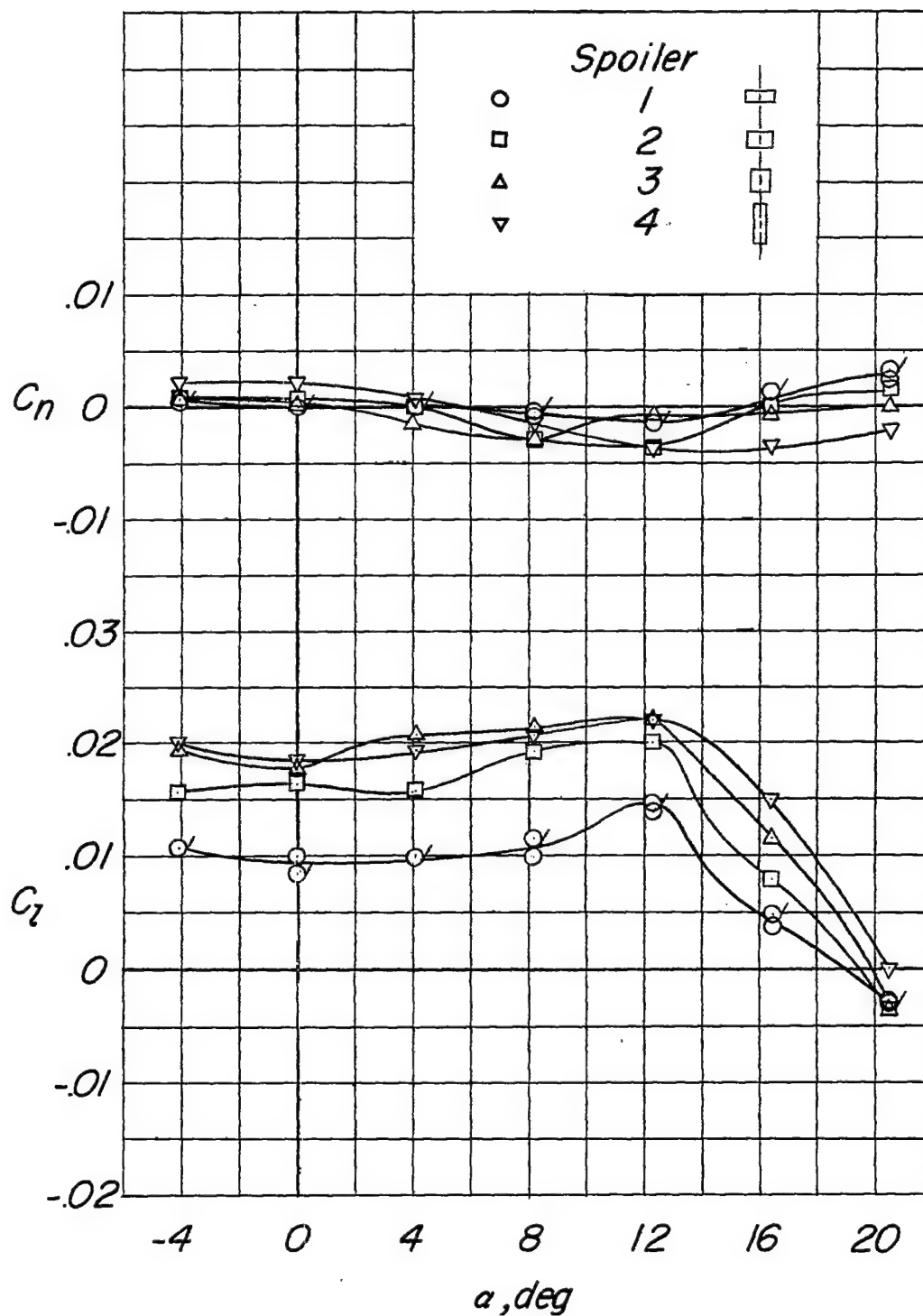


Figure 9.- Lateral-control characteristics of plain spoilers installed on a 60° delta wing. $M = 0.2$. (Data presented for "right-roll" condition. Flagged symbols indicate check tests.)

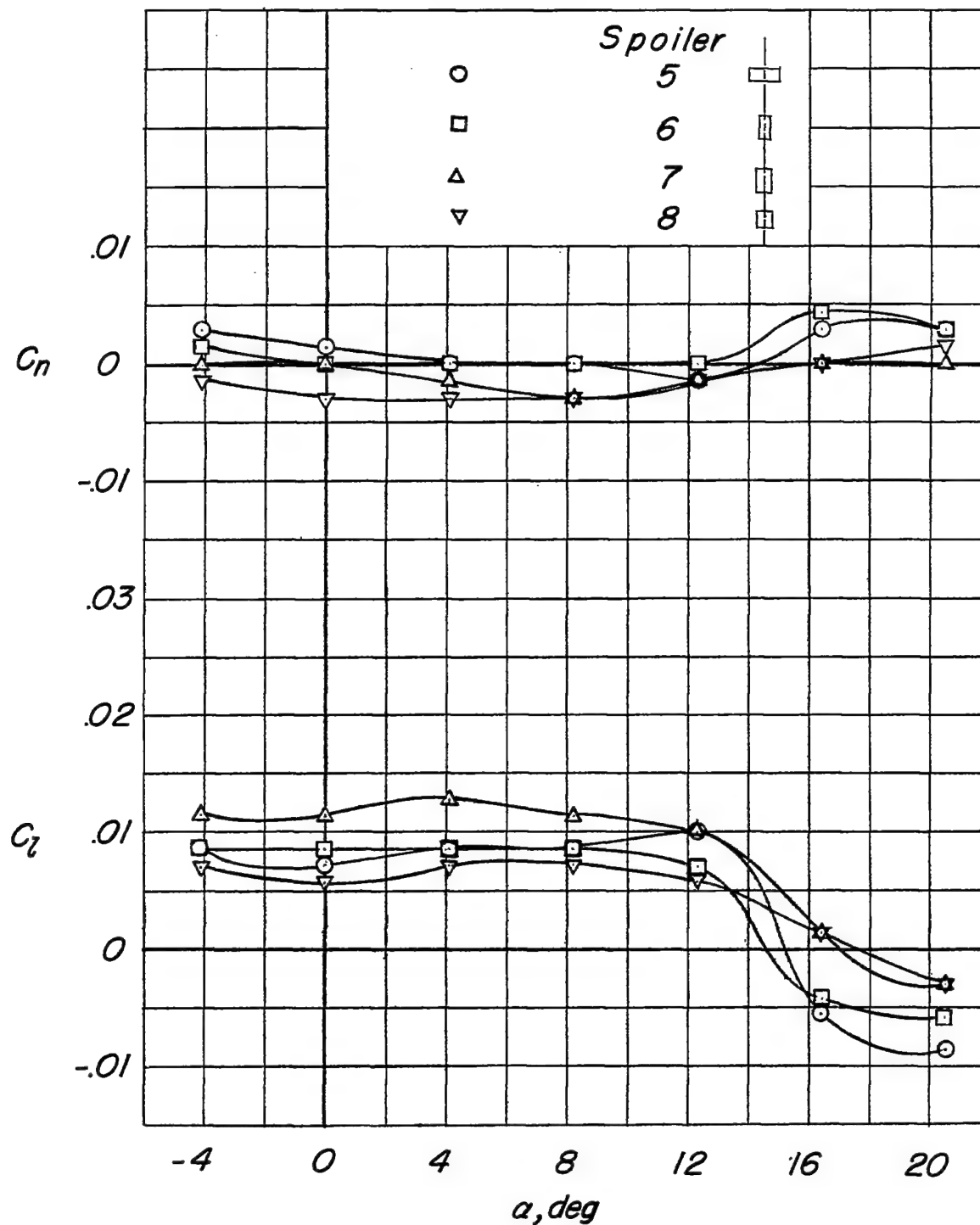


Figure 10.- Lateral-control characteristics of cambered spoilers installed on a 60° delta wing. $M = 0.2$. (Data presented for "right-roll" condition.)

Spoiler

5



6



7



8

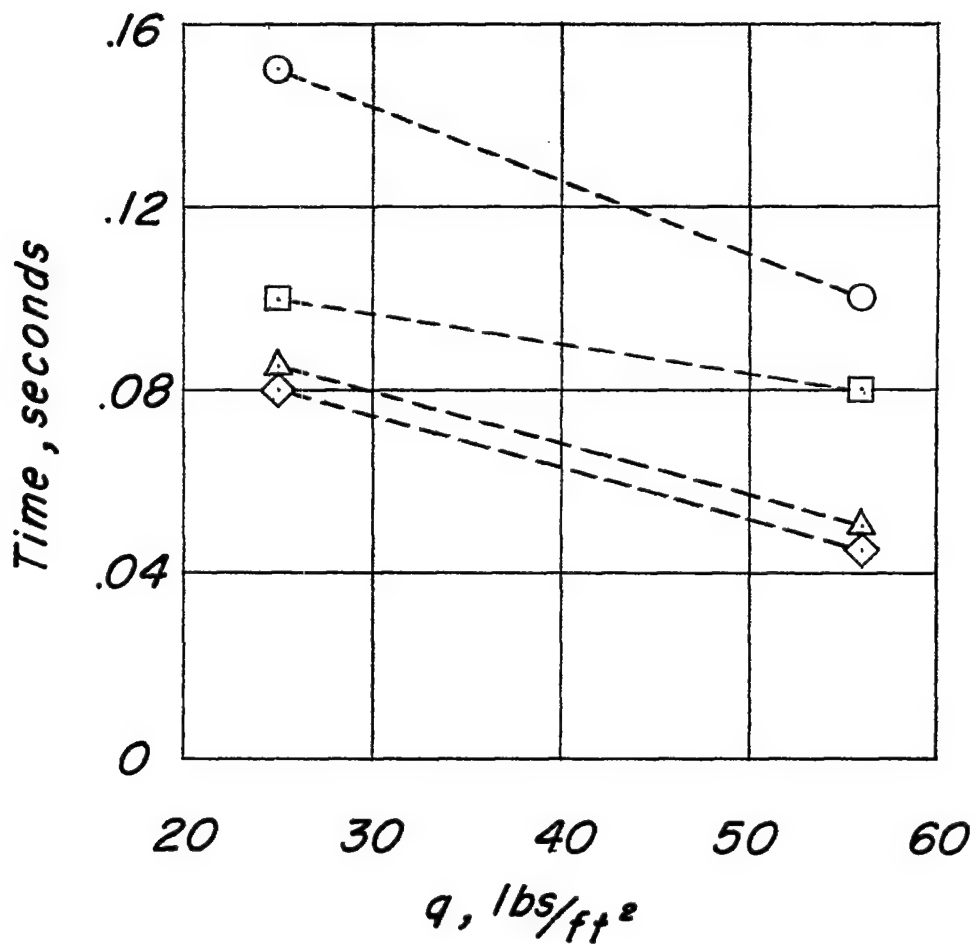
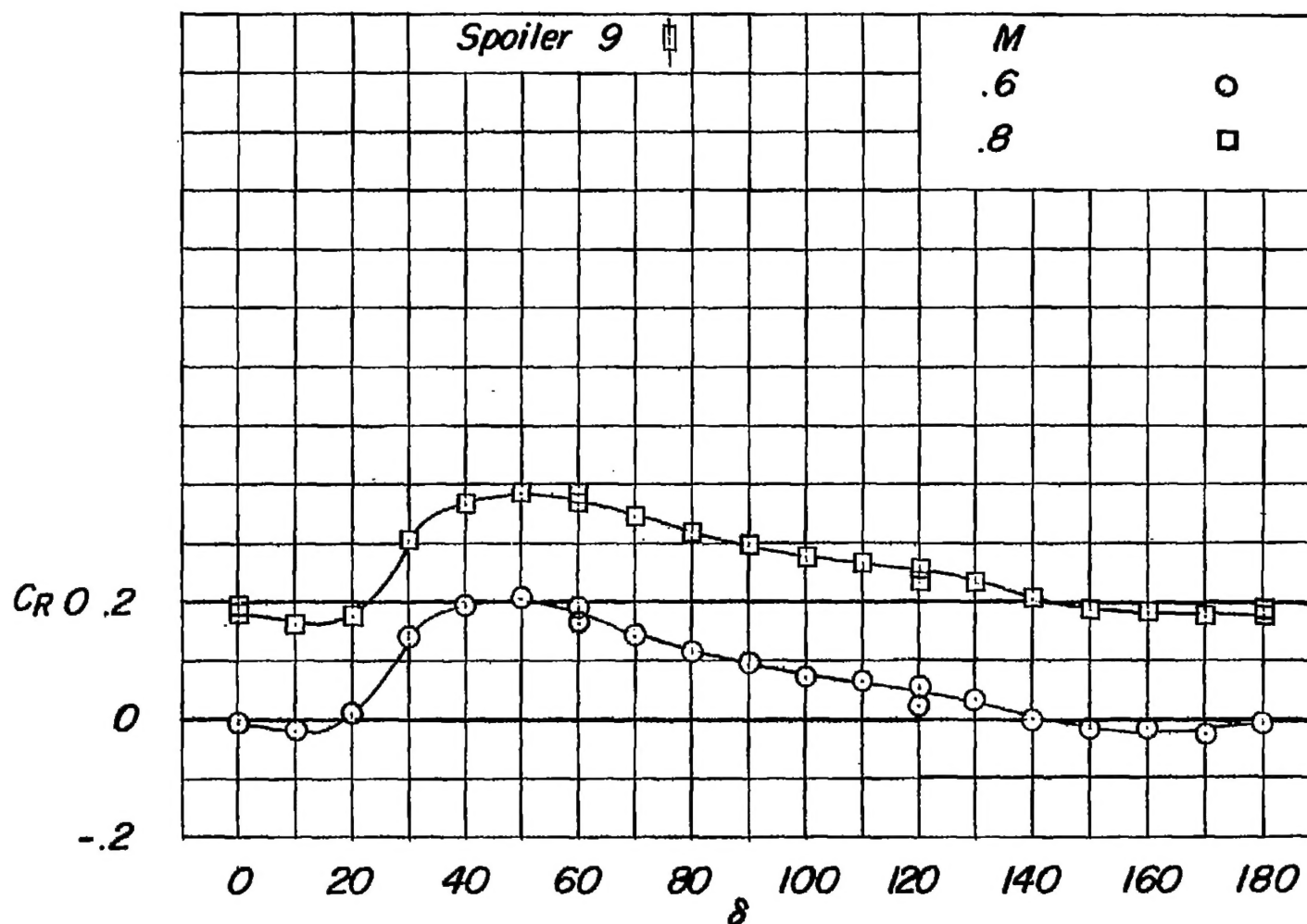
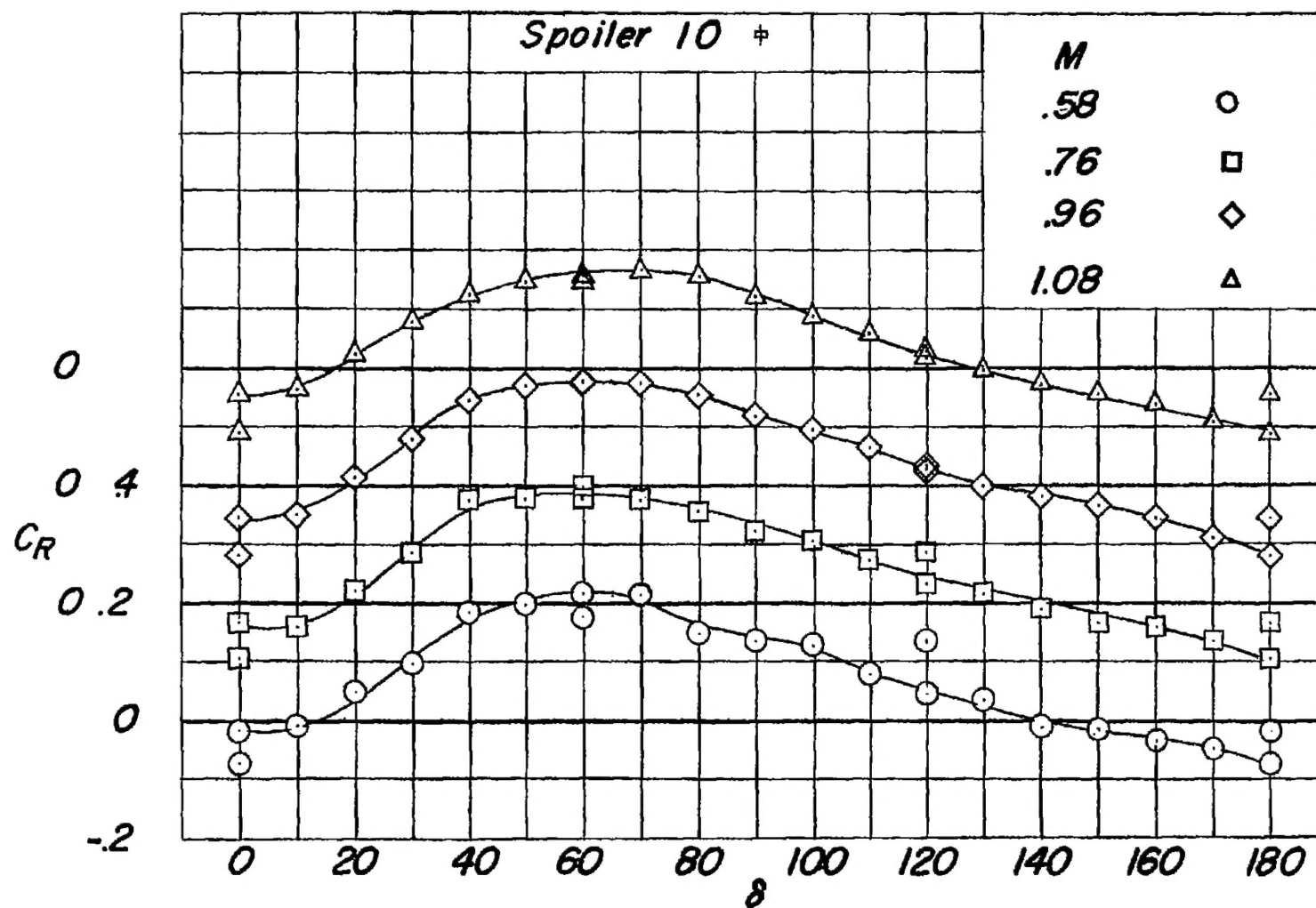


Figure 11.- Variation of time of 90° of rotation from "off" position with dynamic pressure for cambered spoilers tested at low speeds on a 60° delta wing.



(a) Spoiler 9.

Figure 12.- Variation of rotational-moment coefficient with angle of spoiler rotation for spoilers mounted on transonic bump.



(b) Spoiler 10.

Figure 12.- Concluded.

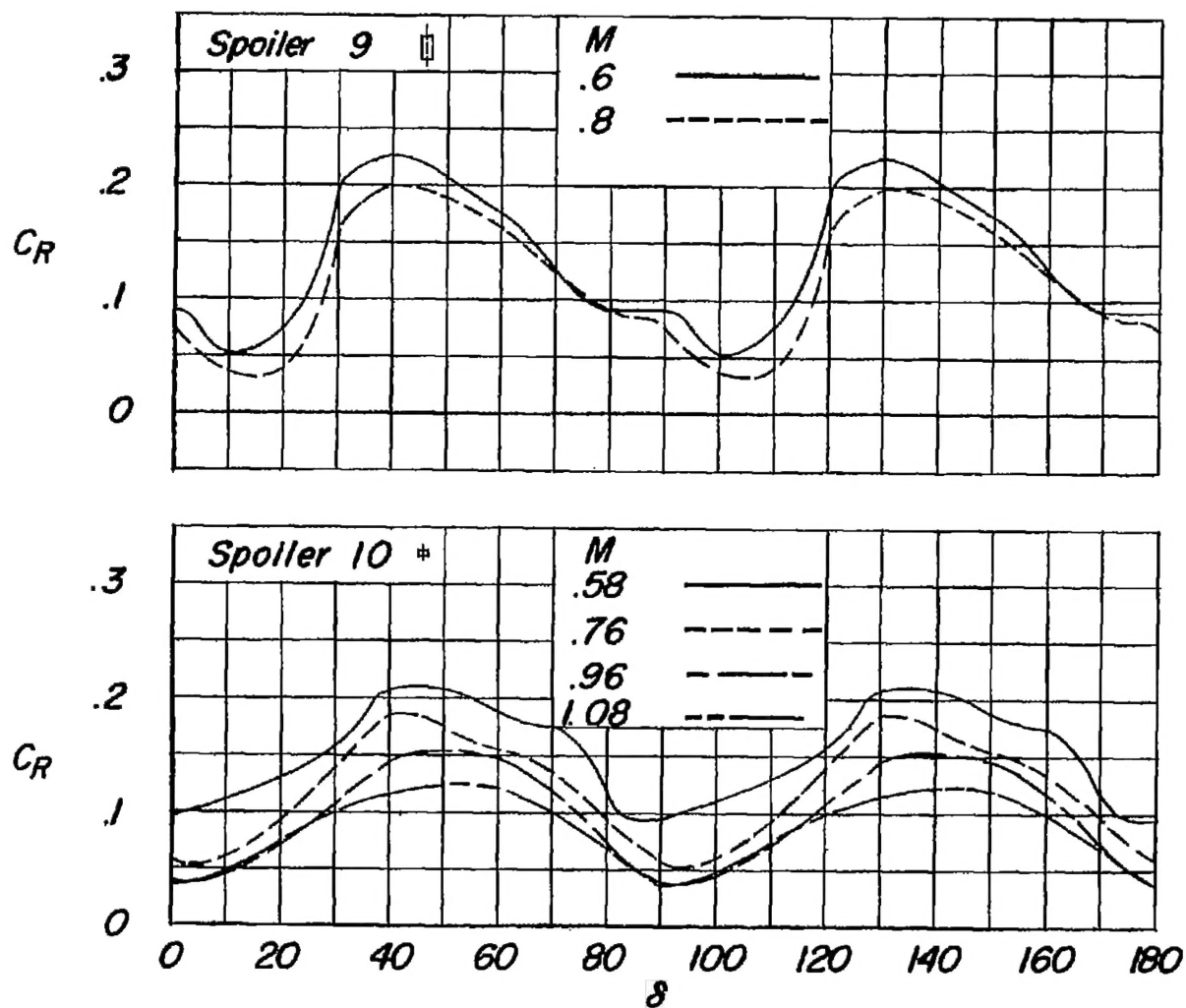


Figure 13.- Summation of the variation of rotational-moment coefficient with angle of rotation at transonic speeds for spoilers considered to be mounted on upper and lower surfaces of wing.

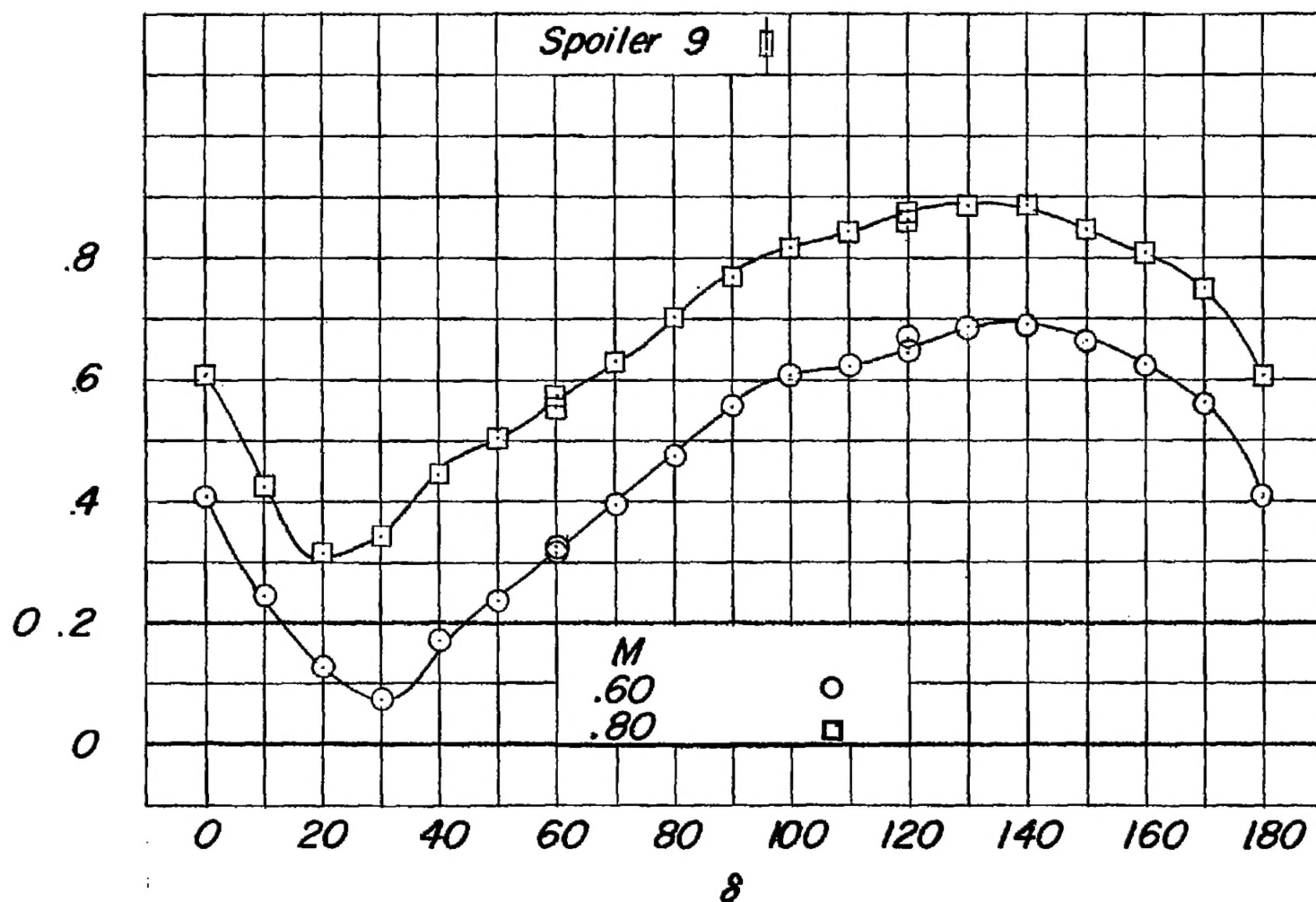


Figure 14.- Variation of bending-moment coefficient with angle of rotation for spoiler mounted on transonic bump.